SDC OPEN

RETINAL LAYER RESPONSE TO RANIBIZUMAB DURING TREATMENT OF DIABETIC MACULAR EDEMA

Thinner is Not Always Better

ANDREAS EBNETER, PHD, MD,*† SEBASTIAN WOLF, PHD, MD,*† JAIN ABHISHEK, MD,* MARTIN S. ZINKERNAGEL, MD, PHD*†

Purpose: To identify individual retinal layer thickness changes associated with visual acuity gain in diabetic macular edema treated with ranibizumab using layer segmentation on high-resolution optical coherence tomography scans.

Methods: Retrospective observational case series. Thirty-three treatment-naive eyes with diabetic macular edema were imaged by spectral domain optical coherence tomography at monthly visits while receiving intravitreal ranibizumab treatment as needed, guided by visual acuity. Thickness changes of individual layers after 1 year were quantitatively analyzed and correlated with visual acuity gain.

Results: The mean best-corrected visual acuity improvement at 1 year was 6.2 (SEM ± 1.5) Early Treatment Diabetic Retinopathy Study letters, and central retinal thickness decreased by 66 ± 18 μm. In the central subfield, there was a significant decrease of thickness for all layers ($P < 0.05$) except the outer nuclear layer. Multiple linear regression analysis revealed that thickness decrease of the inner retina was associated with better visual acuity, whereas for the outer retina the opposite was true. The best estimate of final visual acuity ($R^2 = 0.817$, $P < 0.001$) was obtained, by including baseline visual acuity and thickness change of the inner and outer plexiform layers in the model.

Conclusion: Whereas thickness decrease of the inner retina was positively associated with visual acuity gain, the opposite was found for the outer retina. This might be indirect evidence for recovery of the outer retina during ranibizumab treatment.

RETINA 0:1–10, 2015

Diabetic retinopathy is the most common microvascular pathology in patients with diabetes. It is the leading cause of blindness in working aged adults.[1,2] Among patients with diabetic retinopathy, diabetic macular edema (DME) is the most frequent cause of vision impairment and affects nearly 30% of patients who have diabetes for at least 20 years.[3] Prolonged hyperglycemia is the major etiologic driver of all microvascular changes leading to DME. The cellular mechanisms include thickening of the basement membrane of the retinal capillaries, loss of intramural pericytes, breakdown of the blood retina barrier as evident from opening of the tight junctions, and chronic microvascular inflammation with leukocyte-mediated injury.[4] This disruption of the blood–retina barrier leads to intraretinal accumulation of fluid and plasma constituents such as lipoproteins.

In the last 20 years, noninvasive retinal imaging by low-coherence interferometry has become an indispensable tool in the diagnosis of retinal diseases, as it allows real-time visualization of the retina in great morphological detail. The recent introduction of spectral domain

From the *Department of Ophthalmology, Inselspital, Bern University Hospital and University of Bern, Switzerland; and †Department of Clinical Research, University Hospital Bern, Switzerland.

None of the authors have any financial/conflicting interests to disclose.

Supplemental digital content is available for this article. Direct URL citations appear in the printed text and are provided in the HTML and PDF versions of this article on the journal's Web site (www.retinajournal.com).

Reprint requests: Martin S. Zinkernagel, MD, PhD, University Hospital Bern, 3010 Bern, Switzerland; e-mail: m.zinkernagel@gmail.com

optical coherence tomography has improved the understanding of the pathologic changes and related causes of vision loss in many retinal diseases such as DME.[5–7] With the introduction of anti-vascular endothelial growth factor (anti-VEGF) agents for the treatment of DME, total retinal thickness has often been used in clinical trials as quantitative endpoint to monitor treatment effectiveness.[8–11] However, diabetes is primarily a microvascular disease and as such first leads to alterations in the vascular supply and ischemia, which eventually may result in macular swelling and vision impairment. Because the retina is supplied by two different vascular beds, namely the central retinal artery with its end arteries and the choroidal circulation by diffusion, there exists a watershed zone in the retina and individual retinal layer changes might serve as a biomarker for response to treatment.[12] In this context, a recent report found an association between choroidal thickness and the short-term response to anti-VEGF treatment,[13] and morphological evidence of foveal ganglion cell damage in patients with ischemic damage has been reported.[14] Using fully automated segmentation software, we analyzed individual retinal layers in treatment-naive eyes at baseline and after 1 year of continuous treatment with ranibizumab. After the initial loading phase consisting of at least 3 monthly intravitreal injections until stability was reached, retreatment was administered as needed, guided by visual acuity.

The investigated parameters might serve as useful biomarkers to monitor intravitreal anti-VEGF treatment for DME in daily practice and future clinical trials.

Methods

This study is a retrospective single-center observational case series. Ethics approval (KEK-Nr. 093/13) was granted by the ethics committee of the University of Bern, Switzerland, which works in accordance with International Conference on Harmonisation of Good Clinical Practice guidelines. The need for individual written consent was waived because of the retrospective nature of the project.

Participants

One eye of consecutive adult diabetic patients treated at our institution for center-involving DME and deterioration of visual acuity requiring treatment with anti-VEGF (ranibizumab) were included in this analysis. If both eyes of a patient fulfilled the criteria for inclusion, one eye was chosen randomly. All patients had spectral domain optical coherence tomography and fluorescein angiography at baseline. Nine eyes had concomitant ischemic maculopathy as defined previously.[15] Only eyes naive to intravitreal drug application at baseline with at least one year of continuous ranibizumab treatment and follow-up were included from the procedures log of the Retinal Service of the Department of Ophthalmology at the University Hospital Bern, Switzerland. Exclusion criteria included previous macular laser, uncontrolled glaucoma, or a history of intravitreal steroids. The loading protocol was identical for all patients and consisted of $\geq$3 monthly intravitreal injections of ranibizumab 0.5 mg/0.05 mL until visual stability was attained. Treatment was then suspended but reinitiated if signs of new activation were detected, applying the RESTORE stability and retreatment criteria.[16]

In addition to spectral domain optical coherence tomography imaging, best-corrected visual acuity (BCVA) was tested at baseline and monthly thereafter on the Early Treatment Diabetic Retinopathy Study (ETDRS) charts at 4 meters.

Image Acquisition

Spectral domain optical coherence tomography (Spectralis HRA + OCT; Heidelberg Engineering GmbH, Heidelberg, Germany) scans were serially acquired in tracking mode using an established protocol consisting of both a crosshair and a volume scan. The volume scan, covering 20° × 20°, comprised 49 parallel B-scans separated by 120 μm, whereby each B-scan was the average of 9 frames (automated real time repetition rate = 9), each consisting of 512 A-scans. For retinal layer segmentation, the Heidelberg Eye Explorer software (Version 1.9.10.0; Heidelberg Engineering GmbH, Heidelberg, Germany) was used. The provided standard ETDRS grid with central subfield (r = 0.5 mm), inner ring (r = 0.5–1.5 mm), and outer ring (r = 1.5–3 mm) was used for calculation of the mean thickness of each retinal layer within the corresponding areas. The Heidelberg Eye Explorer recognizes 11 different retinal tissue interfaces: the inner limiting membrane, the boundaries between the retinal nerve fiber layer and the ganglion cell layer (GCL), between the GCL and the inner plexiform layer (IPL), between the IPL and the inner nuclear layer (INL), between the INL and the outer plexiform layer (OPL), between the OPL and the outer nuclear layer (ONL), the external limiting membrane, the ellipsoid zone, the interdigitation zone, the retinal pigment epithelium (RPE), and Bruch's membrane with the underlying choroid. These landmarks allow the software to handle the following retinal layers: retinal nerve fiber layer, GCL, IPL, INL, OPL, ONL, and the photoreceptor–RPE complex. Based on the metabolic supply, the inner retina has been defined as the summation of retinal nerve fiber layer, GCL, IPL,

and INL for some analyses in this study. The sum of the remaining three layers (OPL, ONL, the photoreceptor–RPE complex) is referred to as outer retina throughout this article. Two experienced retina specialists reviewed the retinal layer segmentation of each spectral domain optical coherence tomography volume scan, and segmentation lines were manually corrected.

Statistical Analysis

Study data were collected and managed using the REDCap electronic data management tool hosted at the Department of Ophthalmology, Bern University Hospital, Switzerland.[17] The last observation carried forward method was used to substitute missing visual acuity data. For statistical analysis, a commercial software package (Prism 6; GraphPad Software Inc, La Jolla, CA) was used. Serial changes were analyzed using the Wilcoxon matched-pairs signed-rank test or a paired Student's *t*-test, depending on the distribution. Possible predictive factors of BCVA at the last follow-up and letter gain were identified by bivariate Pearson correlation analysis. Subsequently, multivariate analysis (ordinary least squares linear regression with stepwise forward elimination) was performed with R (Version 3.2.1) to confirm parameters significantly associated with visual outcome.[18–20] The number of intravitreal injections, baseline BCVA, and 1-year thickness decrease of all retinal layers were included as potential explanatory variables. In the manuscript, means are given with the standard error. All tests were 2-sided and P values < 0.05 were regarded as statistically significant.

Results

Thirty-three patients with treatment-naive DME that were started on intravitreal ranibizumab were included in this study. The mean age ±SEM of patients at initiation of treatment was 63.6 ± 2.1 years. The gender distribution (20 males, 13 females) was deemed acceptable and without influence on results. The mean BCVA at baseline was 59.9 ± 2.8 ETDRS letters and increased by an average of 6.2 ETDRS letters to 66.1 ± 2.7 at month 12 ($P < 0.001$; Figure 1A). Central retinal thickness decreased from 425 ± 21 μm at baseline to 359 ± 20 μm at month 12 ($P < 0.001$; Figure 1B). The average total retinal thickness in the inner ring decreased from 408 ± 15 μm at baseline to 366 ± 14 μm at one year ($P < 0.001$) and in the outer ring from 345 ± 11 μm to 326 ± 9 μm ($P < 0.001$; Figure 1C). On average, patients received 6 intravitreal injections of ranibizumab in the first year of treatment.

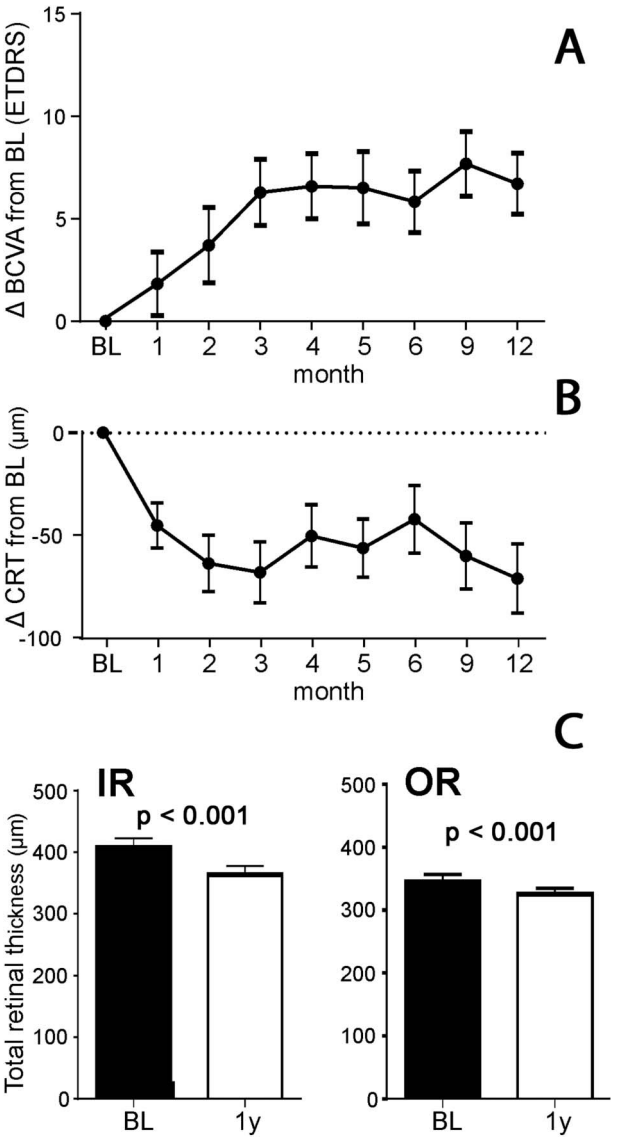

Fig. 1. Visual acuity gain and reduction of central retinal thickness. Mean change (±SEM) in BCVA from baseline (BL) to month 12 in ETDRS letters (**A**). Mean change (±SEM) in central retinal thickness (CRT) during treatment (**B**). Mean retinal thickness at baseline and 12 months (1 year) in the inner ring (IR) and the outer ring (OR) of the standard ETDRS grid (**C**). Paired 2-sided Student's *t*-test.

We analyzed the retinal layer segmentation data (representative example in Figure 2A) to assess whether particular layers differed in their response to ranibizumab treatment. Within the ETDRS grid, there was a significant decrease of thickness in most layers (Figure 2B). Of note, the ONL did not show a significant decrease in thickness in the central subfield ($P = 0.256$). Figure 3 illustrates the situation for the IPL and OPL in the inner and outer rings.

Associations of individual layer changes and other potentially important explanatory variables were explored in correlation matrices (Figure 4). Since the

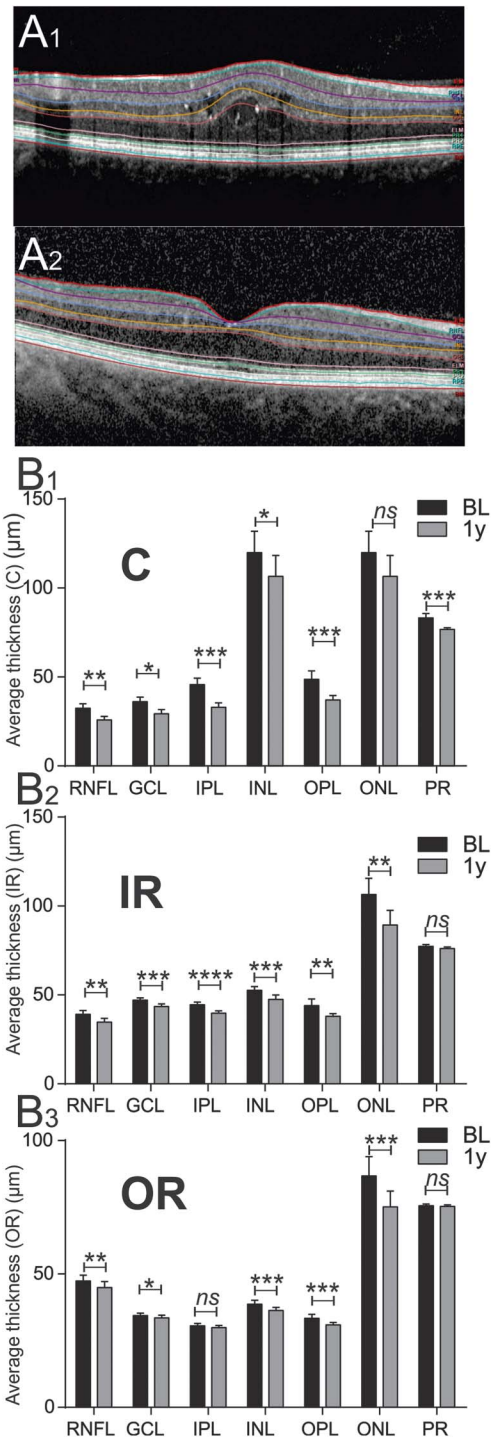

Fig. 2. Retinal layer thickness changes. Representative optical coherence tomogram scans showing layer segmentation at baseline (BL) ($\mathbf{A_1}$) and at one-year (1 year) follow-up ($\mathbf{A_2}$). Retinal layer thickness at BL and after 12 months of continuous treatment in the central subfield (C; $\mathbf{B_1}$), the inner ring (IR; $\mathbf{B_2}$), and the outer ring (OR; $\mathbf{B_3}$) of the ETDRS grid. RNFL, retinal nerve fiber layer; GCL, ganglion cell layer; IPL, inner plexiform layer; INL, inner nuclear layer; OPL, outer plexiform layer; ONL, outer nuclear layer; PR, photoreceptor–RPE complex (Bruch membrane to external limiting membrane). Two-sided paired Student's *t*-test and Wilcoxon matched-pairs signed-rank test (ns: $P > 0.05$; *$P \leq 0.05$; **$P \leq 0.01$; ***$P \leq 0.001$; ****$P \leq 0.0001$).

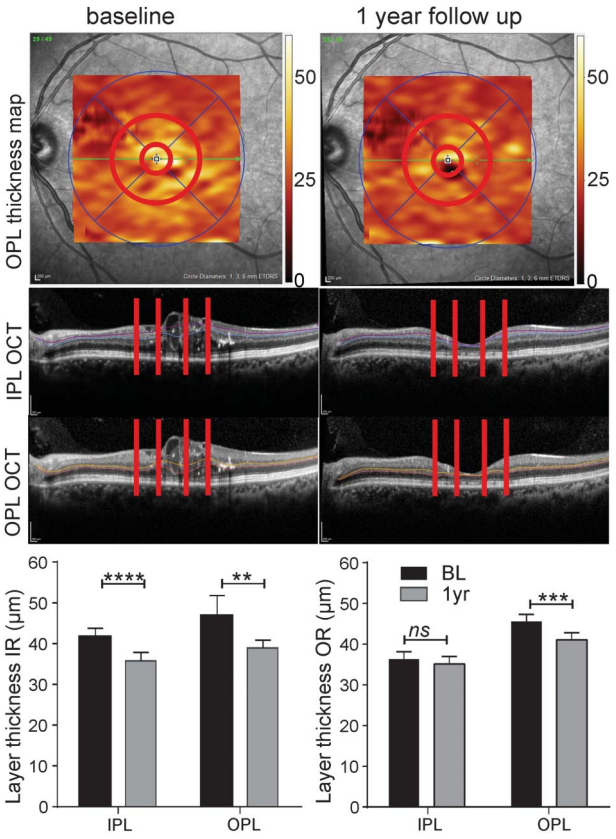

Fig. 3. Response of the inner and outer plexiform layers. **Top**: Quantitative thickness maps at baseline (BL) and at 1 year of treatment (1 year) for the outer plexiform layer (OPL) within the standard ETDRS grid. **Middle**: Corresponding optical coherence tomography scans (red lines delineate the inner ring (IR) of the ETDRS grid) for OPL and inner plexiform layer (IPL). **Bottom**: Bar graphs showing the average thickness (±SEM) of the IPL and OPL at different time points in the IR and the outer ring (OR). Two-sided paired Student's *t*-test and Wilcoxon matched-pairs signed-rank test (ns: $P > 0.05$; **$P \leq 0.01$; ***$P \leq 0.001$; ****$P \leq 0.0001$).

strongest correlations with final visual acuity were found for the central subfield (Figure 4A) and the inner ring (Figure 4B), multivariate analysis was conducted for these subsets of data.

Interestingly, the univariate analysis (Pearson correlation) consistently indicated that decreasing thickness of inner retina layers during treatment was associated with better final BCVA, whereas for the outer retina the relationship was in reverse, in particular in the central ETDRS subfield. These findings were confirmed in multiple linear regression (Tables 1 and 2). However, the strongest influence on final BCVA had baseline BCVA, contributing more than half to the coefficient of determination. The best multivariate linear model (Table 1A) to predict final BCVA included, apart from baseline BCVA, thickness decrease of the IPL and OPL in the central subfield. The coefficient of determination R^2 for this model was 0.817. The excellent fit ($P < 0.001$) is also evident in the model diagnostics analysis

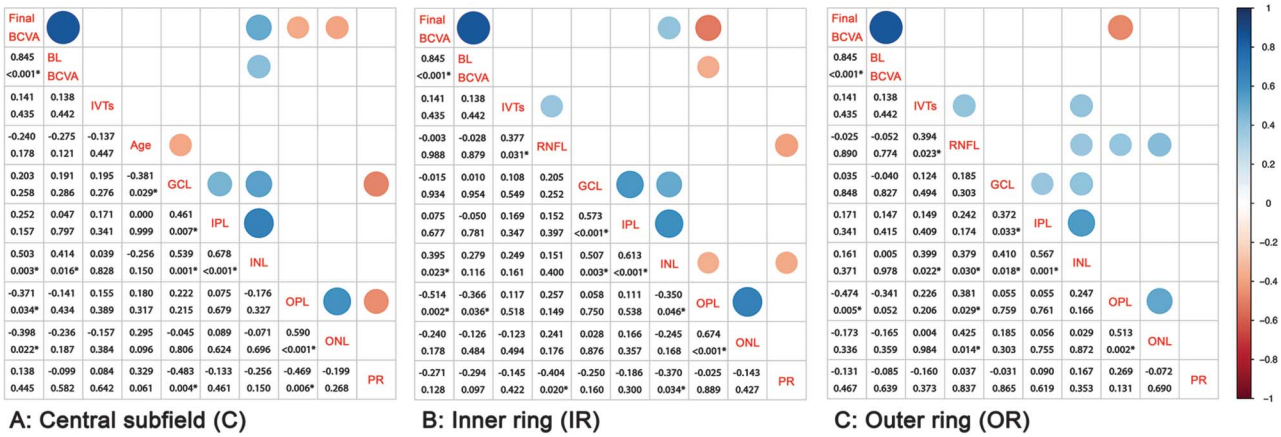

Fig. 4. Correlation plots for individual layer thickness decrease and other parameters. Graphical display of correlation matrices (Pearson's r) for analyzed parameters in specified areas: final BCVA, BL BCVA, number of IVTs, layer thickness decrease for RNFL, GCL, IPL, INL, OPL, ONL, PR. Pair-wise correlations are presented numerically with Pearson's r and corresponding *P* value (below diagonal), and color-size coded (above diagonal) according to the legend on the right. Only significant correlations are shown graphically (significance level $P < 0.05$) and significant *P* values are marked with *. BL, Baseline; IVTs, intravitreal injections; RNFL, retinal nerve fiber layer; PR, photoreceptor–RPE complex.

(see **Figure, Supplemental Digital Content 1**, http://links.lww.com/IAE/A414). Multivariate analysis was also conducted for the ETDRS letter score change (Table 3), with similar results. All models were also calculated excluding baseline BCVA to better dissect the influence of the individual retinal layers.

Discussion

Regular intravitreal treatment with ranibizumab has been shown to result in reduced central retinal thickness and improved BCVA in eyes with DME.[16] Interestingly, in the current retrospective study, visual acuity improvement was negatively associated with the decrease of thickness of the outer retina. At first glance, this seems paradoxical. Anti-VEGFs are most effective at blocking VEGF, arguably the most potent mediator of blood–retina barrier breakdown,[21] and restore capillary integrity reliably. Reduced vascular leakage results in resolution of retinal fluid. Diminished retinal layer thickness would be the obvious consequence, which indeed is observed in most layers and associated with improved visual acuity. How could it be that the outer retina behaves differently from the inner retina? Could this paradox of the outer retina be a sign of neurorecovery?[22]

The metabolic supply of the retina from the central retinal artery has some peculiarities. The inner retina is supplied by four capillary networks that are located in distinct anatomical regions: the nerve fiber layer, the GCL, and the boundaries of the INL towards the IPL and OPL, respectively.[23] The metabolic needs of the outer retina, however, are mostly met by diffusion from the choriocapillaris. The ONL, which contains mainly photoreceptors, the most metabolically active cells in the retina, is a watershed zone and hence prone to hypoxia.[24] In fact, photoreceptors are particularly susceptible to hypoxia[25] and functional deficits are reversible through additional oxygen or glucose supply.[26] The increased diffusion path caused by retinal thickening of the inner layers, the breakdown of the outer blood retina barrier and if present, subretinal fluid, likely deteriorates the metabolic situation of the outer retina.[27,28] In detached retina, the ONL thickness decreases[29] and partially recovers after successful retinal detachment repair in a time-dependent manner.[30] We hypothesize that, in analogy to starving outer retina in retinal detachment, the ONL thickness might decrease in DME. Through improvement of the metabolic supply mediated by resolution of subretinal fluid, restoration of the outer blood retina barrier and drying of the inner layers, viable photoreceptor that have not yet passed the apoptotic threshold might recover and their somata regain their normal size. However, photoreceptors that have already gone into apoptosis will not recuperate and follow their fate to death. This would explain why a decrease of outer retina thickness is negatively associated with better final BCVA. To gain some indirect information on the health of the OPL and ONL in this cohort of patients, it seemed interesting to compare their thickness with normal controls or other pathology with macular swelling. Unfortunately, there are neither data on individual layer thickness in DME nor normative values for elderly individuals published. Comparison was therefore made with some data from younger volunteers (see **Table, Supplemental Digital Content 2**,

Table 1. Central Subfield: Multivariate Forward Stepwise Regression Analysis of Factors With Influence on BCVA at the Last Follow-up in Eyes With DME Treated With Ranibizumab

	Univariate Analysis (Pearson Correlation)		Multivariate Analysis including BL BCVA (Adjusted R^2 = 0.817)*			Multivariate Analysis excluding BL BCVA (Adjusted R^2 = 0.366)*		
A	Correlation Coefficient r	*P*	Unstandardized Regression Coefficient B	Standardized Regression Coefficient β	*P*	Unstandardized Regression Coefficient B	Standardized Regression Coefficient β	*P*
Constant			20.064	—	<**0.001**	63.050	—	<**0.001**
BL BCVA	0.845	<**0.001**	0.766	0.795	<**0.001**			
IVTs	0.141	0.435						
Age	–0.240	0.178						
GCL	0.203	0.258						
IPL	0.252	0.157	0.184	0.236	**0.004**			
INL	0.503	**0.003**				0.259	0.535	**0.001**
OPL	–0.371	**0.034**	–0.182	–0.276	**0.001**			
ONL	–0.398	**0.022**				–0.069	–0.318	**0.036**
PR	0.138	0.445				0.259	0.212	0.167
	Univariate Analysis (Pearson Correlation)		Multivariate Analysis including BL BCVA (Adjusted R^2 = 0.769)*			Multivariate Analysis excluding BL BCVA (Adjusted R^2 = 0.257)*		
B	Correlation Coefficient r	*P*	Unstandardized Regression Coefficient B	Standardized Regression Coefficient β	*P*	Unstandardized Regression Coefficient B	Standardized Regression Coefficient β	*P*
Constant			22.966	—	<**0.001**	65.400	—	<**0.001**
BL BCVA	0.845	<**0.001**	0.716	0.744	<**0.001**			
IVTs	0.141	0.435						
Inner	0.387	**0.026**	0.043	0.184	**0.045**	0.085	0.359	**0.026**
Outer	–0.418	**0.016**	–0.040	–0.216	**0.020**	–0.072	–0.392	**0.016**

*Adjusted coefficient of multiple determination.

Significant *P* values are in bold.

Dependent variable: Final best-corrected visual acuity.

Explanatory variables: Baseline best-corrected visual acuity (BL BCVA), number of intravitreal injections (IVTs), 1-year retinal nerve fiber layer thickness decrease (RNFL), 1-year ganglion cell layer thickness decrease (GCL), 1-year inner plexiform layer thickness decrease (IPL), 1-year inner nuclear layer thickness decrease (INL), 1-year outer plexiform layer thickness decrease (OPL), 1-year outer nuclear layer thickness decrease (ONL), 1-year photoreceptor–RPE-complex (PR) thickness decrease (external limiting membrane to Bruch's membrane).

Model including retinal layers individually (**A**), and aggregated as inner retinal layers (Inner = RNFL + GCL + IPL + INL) and outer retinal layers (Outer = OPL + ONL+PR), respectively (**B**).

Table 2. Inner Ring: Multivariate Forward Stepwise Regression Analysis of Factors With Influence on BCVA at the Last Follow-up in Eyes With DME Treated With Ranibizumab

	Univariate Analysis (Pearson Correlation)		Multivariate Analysis including BL BCVA (Adjusted R^2 = 0.760)*			Multivariate Analysis excluding BL BCVA (Adjusted R^2 = 0.302)*		
A	Correlation Coefficient r	*P*	Unstandardized Regression Coefficient B	Standardized Regression Coefficient β	*P*	Unstandardized Regression Coefficient B	Standardized Regression Coefficient β	*P*
Constant			21.851	—	**<0.001**	70.577	—	**<0.001**
BL BCVA	0.845	**<0.001**	0.732	0.760	**<0.001**			
IVTs	0.141	0.435						
RNFL	–0.003	0.988						
GCL	–0.015	0.934						
IPL	0.075	0.677	0.371	0.142	0.115			
INL	0.395	**0.023**						
OPL	–0.514	**0.002**	–0.230	–0.252	**0.012**	–0.476	–0.522	**0.001**
ONL	–0.241	0.178						
PR	–0.271	0.128				–1.271	–0.284	0.064

	Univariate Analysis (Pearson Correlation)		Multivariate Analysis including BL BCVA (Adjusted R^2 = 0.728)*			Multivariate Analysis excluding BL BCVA (Adjusted R^2 = 0.109)*		
B	Correlation Coefficient r	*P*	Unstandardized Regression Coefficient B	Standardized Regression Coefficient β	*P*	Unstandardized Regression Coefficient B	Standardized Regression Coefficient β	*P*
Constant			21.178	—	**0.001**	68.815	—	**<0.001**
BL BCVA	0.845	**<0.001**	0.773	0.803	**<0.001**			
IVTs	0.141	0.435						
Inner	0.221	0.216						
Outer	–0.369	**0.034**	–0.054	–0.180	0.068	–0.112	–0.369	**0.034**

*Adjusted coefficient of multiple determination.

Significant *P* values are in bold.

Dependent variable: Final best-corrected visual acuity.

Explanatory variables: Baseline best-corrected visual acuity (BL BCVA), number of intravitreal injections (IVTs), 1-year retinal nerve fiber layer thickness decrease (RNFL), 1-year ganglion cell layer thickness decrease (GCL), 1-year inner plexiform layer thickness decrease (IPL), 1-year inner nuclear layer thickness decrease (INL), 1-year outer plexiform layer thickness decrease (OPL), 1-year outer nuclear layer thickness decrease (ONL), 1-year photoreceptor-retinal RPE-complex (PR) thickness decrease (external limiting membrane to Bruch's membrane).

Model including retinal layers individually (**A**), and aggregated as inner retinal layers (Inner = RNFL + GCL + IPL + INL) and outer retinal layers (Outer = OPL + ONL+PR), respectively (**B**).

Table 3. Central Subfield: Multivariate Forward Stepwise Regression Analysis of Factors With Influence on BCVA Gain at the Last Follow-up in Eyes With DME Treated With Ranibizumab

	Univariate Analysis (Pearson Correlation)		Multivariate Analysis including BL BCVA (Adjusted R^2 = 0.480)*			Multivariate Analysis excluding BL BCVA (Adjusted R^2 = 0.388)*		
A	Correlation Coefficient r	*P*	Unstandardized Regression Coefficient B	Standardized Regression Coefficient β	*P*	Unstandardized Regression Coefficient B	Standardized Regression Coefficient β	*P*
Constant			16.556	—	**0.002**	2.686	—	0.176
BL BCVA	–0.341	0.052	–0.209	–0.383	**0.007**			
IVTs	–0.006	0.976						
RNFL	0.245	0.169				0.203	0.298	0.093
GCL	0.007	0.969						
IPL	0.359	**0.041**	0.195	0.440	**0.002**	0.123	0.279	0.099
INL	0.128	0.477						
OPL	–0.395	**0.023**	–0.131	–0.350	**0.025**	–0.109	–0.290	0.077
ONL	–0.268	0.131						
PR	0.424	**0.014**	0.194	0.280	0.069	0.290	0.418	**0.015**

	Univariate Analysis (Pearson Correlation)		Multivariate Analysis including BL BCVA (Adjusted R^2 = 0.285)*			Multivariate Analysis excluding BL BCVA (Adjusted R^2 = 0.044)*		
B	Correlation Coefficient r	*P*	Unstandardized Regression Coefficient B	Standardized Regression Coefficient β	*P*	Unstandardized Regression Coefficient B	Standardized Regression Coefficient β	*P*
Constant			22.966	—	<**0.001**	7.139	—	<**0.001**
BL BCVA	–0.341	0.052	–0.284	–0.519	**0.003**			
IVTs	–0.006	0.976						
Inner	0.221	0.217	0.043	0.324	**0.045**			
Outer	–0.273	0.125	–0.040	–0.381	**0.020**	–0.028	–0.273	0.125

*Adjusted coefficient of multiple determination.

Significant *P* values are in bold.

Dependent variable: Final best-corrected visual acuity.

Explanatory variables: Baseline best-corrected visual acuity (BL BCVA), number of intravitreal injections (IVTs), 1-year retinal nerve fiber layer thickness decrease (RNFL), 1-year ganglion cell layer thickness decrease (GCL), 1-year inner plexiform layer thickness decrease (IPL), 1-year inner nuclear layer thickness decrease (INL), 1-year outer plexiform layer thickness decrease (OPL), 1-year outer nuclear layer thickness decrease (ONL), 1-year photoreceptor-RPE-complex (PR) thickness decrease (external limiting membrane to Bruch's membrane).

Model including retinal layers individually (**A**), and aggregated as inner retinal layers (Inner = RNFL + GCL + IPL + INL) and outer retinal layers (Outer = OPL + ONL+PR), respectively (**B**).

http://links.lww.com/IAE/A415).[31,32] In the eyes with treated DME included in our study, there was some possible thinning of the GCL, IPL and ONL. GCL affection in diabetic patients has been previously described as an early event accompanying hyperglycemia and the lack of insulin,[33] and in association with macular ischemia.[14] Under hypoxic conditions, the ONL thickness may be reduced because of metabolic starvation and shrinkage of cell bodies. The photoreceptor–RPE complex thickness in our patients was not obviously altered, which suggests that the behavior of the ONL cannot be explained by photoreceptor atrophy, which is not an early feature of diabetic retinopathy. Nevertheless, photoreceptors consume a substantial amount of oxygen and may influence the susceptibility to microvascular damage of the other parts of the retina.[34]

To better assess the contribution of the individual retinal layers to the model, baseline BCVA that in fact accounts for more than half of the coefficient of determination, was omitted for subanalysis. Interestingly, instead of the plexiform layers, the nuclear layers were now more relevant as independent variables. It is conceivable, that the health state of the nuclear layers is to some extent represented in baseline BCVA. When this information is no longer directly included in the model, the nuclear layers that implicitly carry information on the health of the neuronal cells in the retina become more influential in the regression model.

At first glance, puzzling is the finding that in the model predicting visual acuity gain, baseline BCVA contributes negatively. However, this finding can be explained by the ceiling effect, i.e., eyes starting with good visual acuity gain fewer letters, because there is less room for improvement. A similar finding has also been reported in other studies, where patients with low visual acuity at baseline gained more letters than patients with better visual acuity at baseline.[35] The finding that a decrease of the photoreceptor–RPE complex height is associated with visual acuity gain can be well explained by the resolution of subretinal fluid.

Limitations of this study include the retrospective design and the small sample size. Moreover, automated segmentation of retina layers in pathologic conditions is not reliable and, in the presence of retinal distortion, prone to artifacts.[36] The software algorithms are manufacturer-specific and differences exist between devices.[37] Review of individual scans and manual correction is necessary, adding a subjective component to the quantification. However, algorithms still work better in conditions with relatively preserved retinal architecture like DME than more destructive degenerative disease such as age-related macular degeneration.[38] Moreover, retrospective analysis of patients treated as needed following a visual acuity-guided regimen carries the risk of positive selection bias.

In conclusion, in this retrospective study we found indirect morphological evidence for neurorecovery of the outer retina during intravitreal treatment of DME with ranibizumab. This recovery is presumably triggered by improved metabolic supply after resolution of intraretinal and subretinal fluid.

Key words: anti-VEGF, diabetic macular edema, layer segmentation, optical coherence tomography, predictive, prognostic, ranibizumab, regression analysis, retina.

References

1. Congdon N, O'Colmain B, Klaver CC, et al. Causes and prevalence of visual impairment among adults in the United States. Arch Ophthalmol 2004;122:477–485.
2. Engelgau MM, Geiss LS, Saaddine JB, et al. The evolving diabetes burden in the United States. Ann Intern Med 2004; 140:945–950.
3. The relationship of glycemic exposure (HbA1c) to the risk of development and progression of retinopathy in the diabetes control and complications trial. Diabetes 1995;44:968–983.
4. Wallow IH, Engerman RL. Permeability and patency of retinal blood vessels in experimental diabetes. Invest Ophthalmol Vis Sci 1977;16:447–461.
5. Browning DJ, Glassman AR, Aiello LP, et al. Optical coherence tomography measurements and analysis methods in optical coherence tomography studies of diabetic macular edema. Ophthalmology 2008;115:1366–1371.
6. Ebneter A, Wolf S, Zinkernagel MS. Prognostic significance of foveal capillary drop-out and previous panretinal photocoagulation for diabetic macular oedema treated with ranibizumab. Br J Ophthalmol In press.
7. Hee MR, Puliafito CA, Duker JS, et al. Topography of diabetic macular edema with optical coherence tomography. Ophthalmology 1998;105:360–370.
8. Brown DM, Nguyen QD, Marcus DM, et al. Long-term outcomes of ranibizumab therapy for diabetic macular edema: the 36-month results from two phase III trials: RISE and RIDE. Ophthalmology 2013;120:2013–2022.
9. Schmidt-Erfurth U, Lang GE, Holz FG, et al. Three-year outcomes of individualized ranibizumab treatment in patients with diabetic macular edema: the RESTORE extension study. Ophthalmology 2014;121:1045–1053.
10. Massin P, Bandello F, Garweg JG, et al. Safety and efficacy of ranibizumab in diabetic macular edema (RESOLVE Study): a 12-month, randomized, controlled, double-masked, multicenter phase II study. Diabetes Care 2010;33:2399–2405.
11. Sivaprasad S, Crosby-Nwaobi R, Esposti SD, et al. Structural and functional measures of efficacy in response to bevacizumab monotherapy in diabetic macular oedema: exploratory analyses of the BOLT study (report 4). PLoS One 2013;8: e72755.
12. Byeon SH, Chu YK, Hong YT, et al. New insights into the pathoanatomy of diabetic macular edema: angiographic patterns and optical coherence tonography. Retina 2012;32: 1087–1099.

13. Rayess N, Rahimy E, Ying GS, et al. Baseline choroidal thickness as a predictor for response to anti-vascular endothelial growth factor therapy in diabetic macular edema. Am J Ophthalmol 2015;159:85–91.
14. Byeon SH, Chu YK, Lee H, et al. Foveal ganglion cell layer damage in ischemic diabetic maculopathy: correlation of optical coherence tomographic and anatomic changes. Ophthalmology 2009;116:1949–1959.
15. Focal photocoagulation treatment of diabetic macular edema. Relationship of treatment effect to fluorescein angiographic and other retinal characteristics at baseline: ETDRS report no. 19. Early Treatment Diabetic Retinopathy Study Research Group. Arch Ophthalmol 1995;113:1144–1155.
16. Mitchell P, Bandello F, Schmidt-Erfurth U, et al. The RESTORE study: ranibizumab monotherapy or combined with laser versus laser monotherapy for diabetic macular edema. Ophthalmology 2011;118:615–625.
17. Harris PA, Taylor R, Thielke R, et al. Research electronic data capture (REDCap)—a metadata- driven methodology and workflow process for providing translational research informatics support. J Biomed Inform 2009;42:377–381.
18. R Core Team. R: A language and environment for statistical computing. R Foundation for Statistical Computing, Vienna, Austria. Available at: http://www.R-project.org/. Accessed August 23, 2015.
19. Venables WN, Ripley BD. Modern Applied Statistics with S. Fourth Edition. New York, NY: Springer, 2002.
20. Taiyun W. Corrplot: Visualization of a Correlation Matrix. R package version 0.73. Available at: http://CRAN.R-project.org/package=corrplot. Accessed November 12, 2014.
21. Ozaki H, Hayashi H, Vinores SA, et al. Intravitreal sustained release of VEGF causes retinal neovascularization in rabbits and breakdown of the blood-retinal barrier in rabbits and primates. Exp Eye Res 1997;64:505–517.
22. Casson RJ, Chidlow G, Ebneter A, et al. Translational neuroprotection research in glaucoma: a review of definitions and principles. Clin Exp Ophthalmol 2012;40:350–357.
23. Tan PE, Yu PK, Balaratnasingam C, et al. Quantitative confocal imaging of the retinal microvasculature in the human retina. Invest Ophthalmol Vis Sci 2012;53:5728–5736.
24. Lange CA, Bainbridge JW. Oxygen sensing in retinal health and disease. Ophthalmologica 2012;227:115–131.
25. Linsenmeier RA. Electrophysiological consequences of retinal hypoxia. Graefes Arch Clin Exp Ophthalmol 1990; 228:143–150.
26. Holfort SK, Klemp K, Kofoed PK, et al. Scotopic electrophysiology of the retina during transient hyperglycemia in type 2 diabetes. Invest Ophthalmol Vis Sci 2010;51:2790–2794.
27. Nguyen QD, Shah SM, Van Anden E, et al. Supplemental oxygen improves diabetic macular edema: a pilot study. Invest Ophthalmol Vis Sci 2004;45:617–624.
28. Qaum T, Xu Q, Joussen AM, et al. VEGF-initiated blood-retinal barrier breakdown in early diabetes. Invest Ophthalmol Vis Sci 2001;42:2408–2413.
29. Dooley I, Treacy M, O'Rourke M, et al. Serial spectral domain ocular coherence tomography measurement of outer nuclear layer thickness in rhegmatogenous retinal detachment repair. Curr Eye Res 2015;40:1073–1076.
30. Menke MN, Kowal JH, Dufour P, et al. Retinal layer measurements after successful macula-off retinal detachment repair using optical coherence tomography. Invest Ophthalmol Vis Sci 2014;55:6575–6579.
31. Demirkaya N, van Dijk HW, van Schuppen SM, et al. Effect of age on individual retinal layer thickness in normal eyes as measured with spectral-domain optical coherence tomography. Invest Ophthalmol Vis Sci 2013;54:4934–4940.
32. Ehnes A, Wenner Y, Friedburg C, et al. Optical coherence tomography (OCT) device independent intraretinal layer segmentation. Transl Vis Sci Technol 2014;3:1.
33. Barber AJ, Lieth E, Khin SA, et al. Neural apoptosis in the retina during experimental and human diabetes. Early onset and effect of insulin. J Clin Invest 1998;102:783–791.
34. Kern TS, Berkowitz BA. Photoreceptors in diabetic retinopathy. J Diabetes Investig 2015;6:371–380.
35. Wells JA, Glassman AR, Ayala AR, et al. Aflibercept, bevacizumab, or ranibizumab for diabetic macular edema. N Engl J Med 2015;372:1193–1203.
36. Ray R, Stinnett SS, Jaffe GJ. Evaluation of image artifact produced by optical coherence tomography of retinal pathology. Am J Ophthalmol 2005;139:18–29.
37. Lammer J, Scholda C, Prunte C, et al. Retinal thickness and volume measurements in diabetic macular edema: a comparison of four optical coherence tomography systems. Retina 2011; 31:48–55.
38. Waldstein SM, Gerendas BS, Montuoro A, et al. Quantitative comparison of macular segmentation performance using identical retinal regions across multiple spectral-domain optical coherence tomography instruments. Br J Ophthalmol 2015;99:794–800.